Shaped Beams from Diamond Field-Emitter Array Cathodes

Andrews, Heather Lynn; Nichols, Kimberley; Kim, Dongsung; Simakov, Evgenya Ivanovna; Antipov, Sergei; Conde, Manoel; Doran, Darrel; Ha, Gwanghui; Liu, Wanming; Power, John; Shao, Jiahang; Whiteford, Charles; Wisniewski, Eric E.; Chen, Gongxiaohui

To be published in: IEEE Transactions on Plasma Science

DOI to publisher's version: 10.1109/TPS.2020.2984156

Shaped Beams from Diamond Field-Emitter Array Cathodes

1st Heather Andrews
LANL
Los Alamos, USA
hlac@lanl.gov

2nd Kimberley Nichols
LANL
Los Alamos, USA

3rd Dongsung Kim
LANL
Los Alamos, USA

4th Evgenya Simakov
LANL
Los Alamos, USA

5th Sergey Antipov
Euclid Techlabs
Bolingbrook, USA

6th Gongxiaohui Chen
IIT
Chicago, USA

7th Manoel Conde
ANL
Lemont, USA

8th Darrel Doran
ANL
Lemont, USA

9th Gwanghui Ha
ANL
Lemont, USA

10th Wanming Liu
ANL
Lemont, USA

11th John Power
ANL
Lemont, USA

12th Jiahang Shao
ANL
Lemont, USA

13th Eric Wisniewski
ANL
Lemont, USA

***Abstract*—Diamond Field-Emitter Arrays (DFEAs) are arrays of diamond pyramids with exquisitely sharp tips and micron scale bases that produce high current densities. These arrays can be fabricated in arbitrary shapes, ranging from single tips to many millions of tips, so that they produce an inherently shaped electron beam. Each tip emits a modest current but large dense array can produce many Amps. We are investigating these cathodes for use in dielectric wakefield accelerators, however they may also be applicable to vacuum microwave tubes. Recently, shaped beam production and transport has been demonstrated in the 1.3 GHz rf gun at the Argonne Cathode Test Stand at Argonne National Laboratory. Charge was measured on a Faraday cup and the beam imaged on a YAG screen with peak electric field gradients on the cathode ranging from 12-35 MV/m. Three cathode geometries were tested: one 1 mm equilateral triangle with 7 micron base pyramids and 10 micron pitch, one 1 mm equilateral triangle with 10 micron base and 25 micron pitch and one sparse 5x5 square array with 20 micron base and 400 micron pitch. The two triangular arrays emitted 35 nC in an rf macropulse at 35 MV/m and 13 nC charge at 27 MV/m respectively, while the sparse array emitted 0.060 nC charge at 15 MV/m. This paper presents results of the triangular array experiments including damage due to breakdown in the rf gun and initial models of tip-to-tip shielding.**

***Index Terms*—field-emission, UNCD, diamond, RF-gun, patterned beam, shaped beam, shielding**

I. Introduction

Transversely shaped beams are broadly interesting for a number of applications. Possible applications include nano-electronics, rf guns, diodes, terahertz devices, and certain free-electron lasers [1]–[5] . We are presently developing inherently shaped beams for use with the emittance exchange (EEX) technique proposed at Los Alamos National Laboratory (LANL) and recently developed at Argonne National Laboratory (ANL) [6]–[9]. The EEX produces temporal shaped beams from transversely shaped beams, for increasing the efficiency of dielectric wakefield acceleration.

Current methods to produce transversely shaped beams include using a photocathode excited by a patterned drive laser beam [10], and using an intercepting mask on the electron beam [7], [8], [11]. The disadvantages of the mask method include hazardous x-rays, produced when the mask intercepts the beam, beam loss onto the mask of up to 80%, and inconsistency in the beam shape shot-to-shot due to jitter. One can overcome these disadvantages by creating a cathode that produces an intrinsically shaped electron beam. Additionally, using a field-emission cathode eliminates the need for a drive laser, simplifying overall gun design.

LANL has recently developed the capability to produce Diamond Field-Emitter Array (DFEA) cathodes [15]. These cathodes are arrays of pyramids having nanoscale tips, with base sizes ranging from 3 μm to 25 μm, and pitches of 5 μm and greater. While DFEAs have been investigated for a number of years at other institutions [16], [17], LANL currently has a program studying these cathodes in a 40 kV dc test stand. Fig. 1 shows the SEM images of dense triangular DFEA cathodes, with the insets showing different magnifications. Cathode fabrication is based on standard silicon wafer techniques, allowing production of arrays with nearly arbitrary geometric shapes. In this paper we present initial results from the two dense triangular DFEA cathodes that were tested in the rf gun at the Argonne Cathode Teststand (ACT) facility at ANL [12]–[14] as well as initial

The authors gratefully acknowledge the support of Los Alamos National Laboratory (LANL) Laboratory Directed Research and Development (LDRD) program. This work was performed, in part, at the Center for Integrated Nanotechnologies, an Office of Science User Facility operated for the U.S. Department of Energy (DOE) Office of Science. Los Alamos National Laboratory, an affirmative action equal opportunity employer, is managed by Triad National Security, LLC for the U.S. Department of Energy?s NNSA, under contract 89233218CNA000001. The work at AWA is funded through the U.S. Department of Energy Office of Science under Contract No. DE-AC02-06CH11357.

simulations of tip-to-tip shielding. Results from the sparse array tests, which successfully demonstrated production and transport of a patterned beam from a field-emission cathode in an rf gun, along with initial estimates of per-tip current and emission area, are reported elsewhere [18]. Earlier steps in this work have been reported in [19], [20]

II. Experimental Test Setup

A schematic of the ACT set-up is shown in Fig. 2. The test stand consists of a 0.5-cell L-band 1.3 GHz rf gun, followed by several beamline diagnostics including: gun solenoids, Gsol1 and Gsol2, a beamline solenoid, Bsol, two Faraday cups, FC1 and FC2, and three YAG screens, YAG1, YAG2, and YAG3. FC1 is coincident with YAG1, and FC2 is coincident with YAG3, as shown. The rf field in the gun cavity is calculated based on the measured input power. The vacuum level was maintained at or below $2\text{x}10^{-8}$ Torr. Generally during experiments the rf power was increased slowly until emission was observed on YAG1, at which point the gun solenoids were adjusted to maximize the charge capture. The rf power was subsequently increased to a stable operating point, and images could be seen on all three YAG screens. Charge during the rf macropulse as a function of field was measured on the first Faraday cup (FC1), and re-plotted as I-V curves. We tested two dense triangular array cathodes. The first, CAT1, was an equilateral triangle, 1 mm on a side, with 7 μm base pyramids and 10 μm pitch. The second cathode, CAT2, was also an equilateral triangle 1 mm on a side, with 10 μm base and 25 μm pitch. SEM images of CAT1 and CAT2 are shown in Fig. 1. As can be seen in these images, the DFEA pyramids emerge from a flat diamond film about 10 μm thick. This film is brazed onto the molybdenum substrate as shown in Fig. 3, which is then attached to the cathode plug and mounted in the rf gun. In Fig. 3, the black square is the diamond film, and the triangular array can be seen above and slightly left of center of the cathode holder.

III. Experimental Results

Charge in an rf macropulse measured on FC1 is plotted as a function of electric field on the cathode in Fig. 4 (left for CAT1 and right for CAT2). The different colors correspond to different sets of data taken on different days and times. Typically we started testing the cathode at lower cathode fields, working to higher fields. Data were taken starting at the highest field achieved with minimum breakdowns, and collected for descending fields on the cathode to avoid breakdowns during the collection process. The maximum charge measurements of 35 nC at 36 MV/m and 9 nC at 21 MV/m for CAT1 and CAT2 respectively, surpass the sub-nC charge produced in this gun using a copper photocathode [21], which is notable because the gun is far from optimized for a field emission cathode. Another significant point is that the charge for the sparser, slightly larger pyramids, CAT2, is higher for the same field than the charge from the denser smaller pyramids, CAT1, even though there are significantly more tips on CAT1. We have conducted simulations to investigate tip-to-tip shielding, discussed later, and it appears that this explains the difference in emitted charge between the cathode samples.

There were a number of challenges in these tests including difficulty centering the arrays on the cathode plug and sharp edges of the cathode plugs. Fig. 5 shows the image of the beam from CAT1 on YAG2. While there are features that suggest a triangular shape, we did not observe a clear triangle for this sample. Likely a combination of both space charge effects near the cathode and poor array centering with respect to gun center, or more specifically, the magnetic center of the gun solenoids, contributed to this difficulty imaging the beam, especially as it was transported down the beam line.

Sharp cathode plug edges likely contributed to the maximum cathode field gradients that we were able to achieve, because these edges initiated breakdowns in the gun. It is likely that at sufficiently high fields the array may have caused breakdowns, however there was no diagnostic to determine the location of breakdowns observed in the gun region. Breakdowns eventually led to decreased bunch charge from the array in subsequent tests. At the end of the experiment when the arrays were removed from the gun and imaged by SEM, significant damage was observed, as shown for CAT1 in Fig. 6.

IV. Initial Modeling Results

In parallel with the cathode experiments, we have been conducting modeling using the MICHELLE gun code [22]. Emitter simulations were conducted in MICHELLE; individual emitters were modeled to get accurate field enhancement factors and currents similar to the experiment, then interactions between individual emitters were modeled to describe whole-array behavior. The array behavior led to the initial demonstration of shielding effects between emitters. This shielding effect is consistent with previous results [23]. The models are challenging in part because the ratio between the largest and smallest element in the model is around 10000:1, as shown in Fig. 7. Here we see an individual pyramid with the nanometer scale tip represented as a rounded pillar on the top. The pyramid base is 25 μm, and the diameter of the pillar is 20 nm. The largest element in the model has a length of about 14 μm, while the smallest is 1.3 nm. Figure 8 shows modeled electron emission scaled to include the whole pyramid (left) and showing just the sharp tip (right). In the right frame, the equipotential electric field lines are also shown in green.

Fig. 9 shows the geometry used to investigate tip-to-tip shielding. The figure shows two quarter-pyramid emitters of fixed base size and with a variable pitch shown by the red double-headed arrow. The model uses Neuman boundary conditions to emulate an infinite sea of emitters. Emission current data was modeled for pitches from 10 μm to 50 μm, with a constant pyramid height of 5.5 μm (base of 7 μm) and is shown plotted in Fig. 10. This plot agrees roughly with initial experimental data, showing that emitted current increases with array pitch until about 30 μm. Though we do not have good measurements of per tip current, we do observe that bunch charge for a fixed cathode field increases with emitter spacing for pitches of 10-25 μm. Experiments taking place this fall

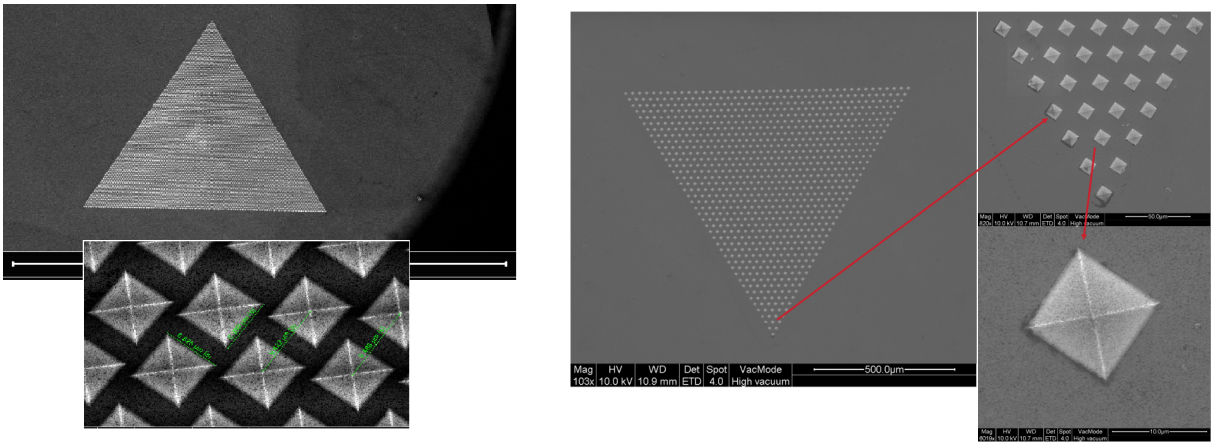

Fig. 1. SEM images of the two triangular arrays at different magnifications. On the left is "CAT1" with 7 μm base, 10 μm pitch, and on the right is "CAT2" with 10 μm base, 25 μm pitch. Both cathode arrays are 1 mm equilateral triangles.

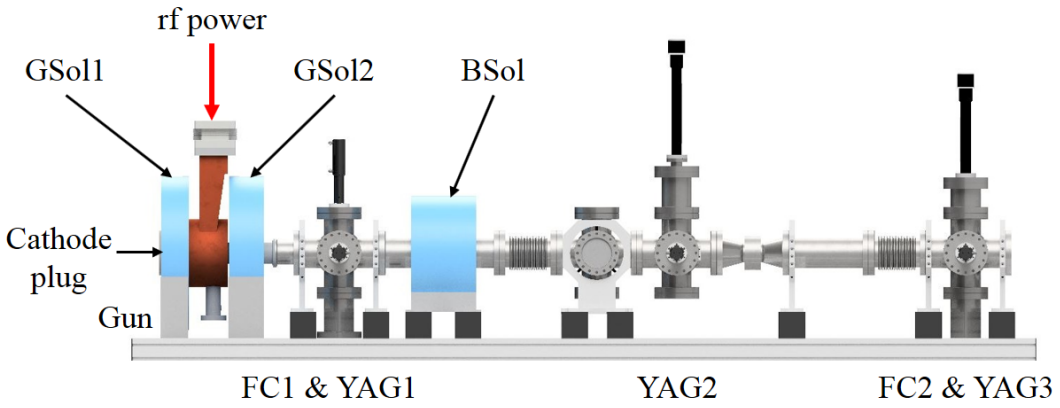

Fig. 2. ACT beamline schematic, where FC1, and YAG1 are coincident, along with FC2, YAG3.

will help confirm these results. A purely geometric argument suggests that once the emitters are more than twice the height apart they should not shield each other, however these initial results suggest that the shielding effect we observe may be more complicated.

V. Conclusion

Initial DFEA cathode tests in an rf gun show great promise; we are able operate inherently shaped field-emitter arrays and achieve high bunch charge. Cathode plug modifications are being made to reduce breakdown from sharp edges, and improved array centering will help patterned beam transport. Further experiments are underway to examine the role of pyramid base size and pitch on emission behavior, continue to investigate tip-to-tip shielding effects, and better understand I-V characteristics and emitter lifetime.

VI. References

References

[1] A. I. Akinwande, "Vacuum Nano Electronics: Back to the Future or Foreword to the Future?" *IVNC Proc.* (2019).

[2] J. W. Lewellen, and J. Noonan, "Field-emission cathode gating for rf electron guns," *Phys. Rev. ST-AB* 8, 033502 (2005).

[3] P. Zhang, A. Valfells, L. K. Ang, J. W. Luginsland, and Y. Y. Lau, "100 years of the physics of diodes," *Appl. Phys. Rev.* 4, 011304 (2017).

[4] J. H. Booske *et al.*, "Vacuum electronic high power terahertz sources," *IEEE THz Sci. and Tech.* 1, 54, (2011).

[5] B. D. Patterson *et al.*, "Coherent science at the SwissFEL x-ray laser, *New J. Phys.* 12 (2010).

[6] D. Y. Shchegolkov and E. I. Simakov, "Design of an emittance exchanger for production of special shapes of electron beam current," *Phys. Rev. STAB* 17, 041301 (2014).

[7] G. Ha *et al.*, "Precision control of the electron longitudinal bunch shape using an emittance-exchange beam line," *Phys. Rev. Lett.* 118, 104801 (2017).

[8] Q. Gao *et al.*, "Observation of high transformer ratio of shaped bunch generated by an emittance-exchange beam line", *Phys. Rev. Lett.*, 120, 114801, (2018).

[9] R. Roussel *et al.*,"Single Shot Characterization of High Transformer Ratio Wakefields in Nonlinear Plasma Acceleration,? *Phys. Rev. Lett.* 124, 044802(2020)

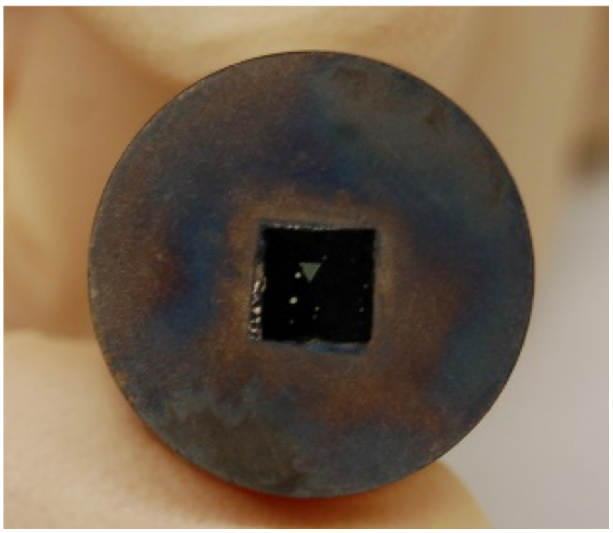

Fig. 3. Photograph of the cathode plug showing the diamond, and triangular array off center within the diamond area. This version of the cathode plug had square edges which caused many breakdowns in the rf gun.

[10] A. Halavanau *et al.*, "Spatial Control of photoemitted electron beams using a microlens-array transverse-shaping technique", *Phys. Rev. AB* 20, 103404 (2017).

[11] G. Ha *et al.*, "Perturbation-minimized triangular bunch for high-transformer ratio using a double dogleg emittance exchange beam line", *Phys. Rev. AB* 19, 121301, (2016).

[12] SV Baryshev *et al.*, "Planar ultrananocrystalline diamond field emitter in accelerator radio frequency electron injector: Performance metrics", *Appl. Phys. Lett.* 105, 203505 (2014).

[13] J Shao *et al.*,"In Situ Observation of Dark Current Emission in a High Gradient rf Photocathode Gun," *Phys. Rev. Lett.* 117, 084801 (2016)

[14] J Shao *et al.*,"High power conditioning and benchmarking of planar nitrogen-incorporated ultrananocrystalline diamond field emission electron source," *Phys. Rev. AB* 22, 123402 (2020)

[15] D. Kim *et al.*, "Fabrication of micron-scale diamond field-emitter arrays for dielectric laser accelerators", *IEEE Adv. Acc. Conc. Workshop 2018*, DOI:10.1109/aac.2018.8659407, (2018).

[16] J. D. Jarvis *et al.*, "Uniformity conditioning of diamond field emitter arrays", *J. Vac. Sci. Technol. B: Microelectron. Nanometer Struct. Process. Meas. Phenom.*, 27, 2264, (2009).

[17] H. L. Andrews *et al.*, "An investigation of electron beam divergence from a single DFEA emitter tip", *IPAC18 Conf. Proc.*, https://doi.org/10.18429/JACoW-IPAC2018-THPML007, (2018).

[18] K. Nichols *et al.*, " Demonstration of transport of a patterned electron beam produced by diamond pyramid cathode in an rf gun," *Appl. Phys. Lett.* 116, 5128109, (2019).

[19] K. E. Nichols *et al.*, "Modeling of Diamond Field Emitter Arrays for Shaped Electron Beam Production," *IPAC18 Conf. Proc.*, https://doi.org/10.18429/JACoW-IPAC2018-THPML010, (2018).

[20] K. E. Nichols *et al.*, "Experimental Results of Dense Array Diamond Field Emitters in RF Gun," *IPAC19 Conf. Proc.*, TUPT090, (2019).

[21] Jiahang Shao, private communications

[22] J. Petillo *et al.*, "The michelle three-dimensional electron gun and collector modeling tool: Theory and design," *IEEE Trans. Plasma Sci.* 30, 1238 (2002).

[23] J. R. Harris, K. L. Jensen, and D. A. Shiffler, "Dependence of optimal spacing on applied field in ungated field emitter arrays," *AIP Advances* 5, 081982 (2015).

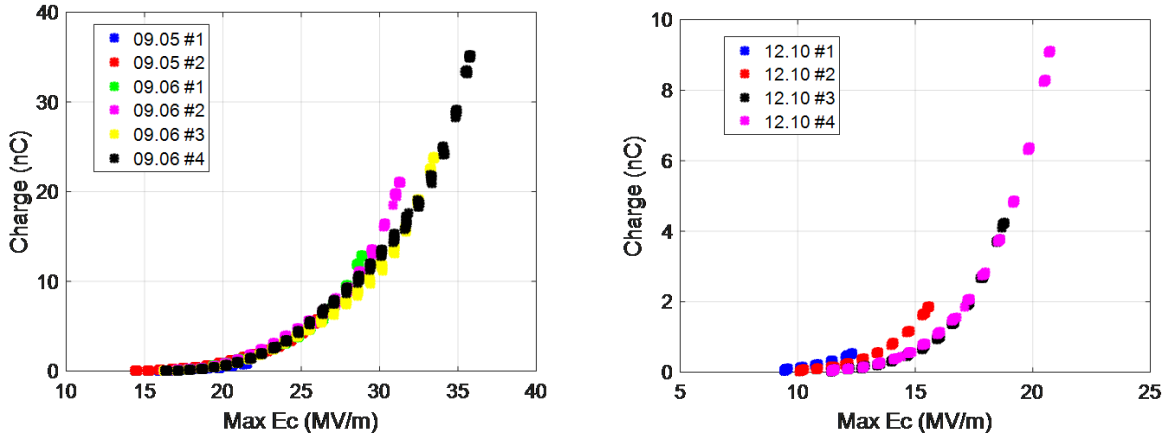

Fig. 4. Charge in an rf macropulse vs. electric field at the cathode for CAT1 (left) and CAT2 (right)

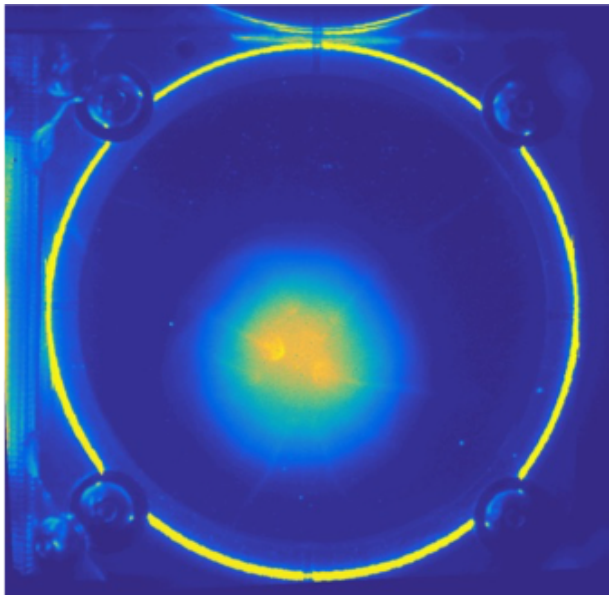

Fig. 5. Image of the beam of YAG2, 1.5 m down the beam line. We did not observe a clear triangular pattern from this sample, most likely due to space charge effects.

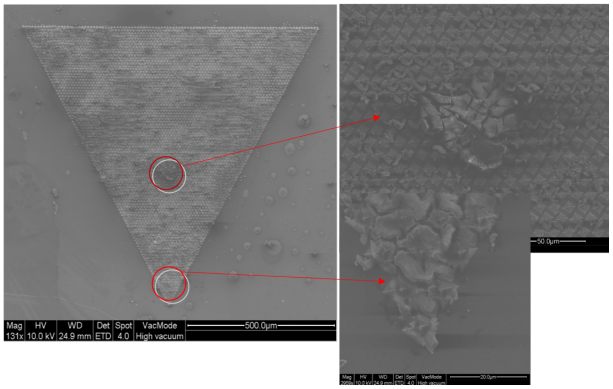

Fig. 6. SEM image of CAT1 after breakdowns in the rf gun. At sufficiently high field, arrays can sustain significant damage.

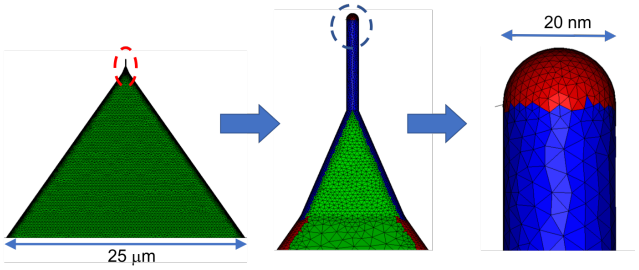

Fig. 7. Mesh details of the pyramid tip simulation, progressively zooming from left to right. Note that the pyramid base can be 25 μm in length while the diameter of the nanotip can be 20 nm, requiring vastly different sizes of mesh elements.

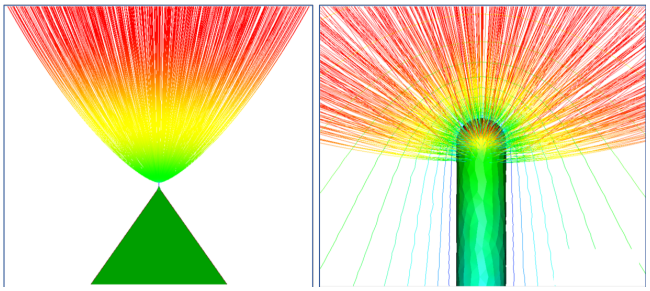

Fig. 8. Emission from a single tip modeled in MICHELLE. The whole pyramid is shown in the left frame, while the right frame shows detail of emission from only the very tip, as well as the green equipotential electric-field lines.

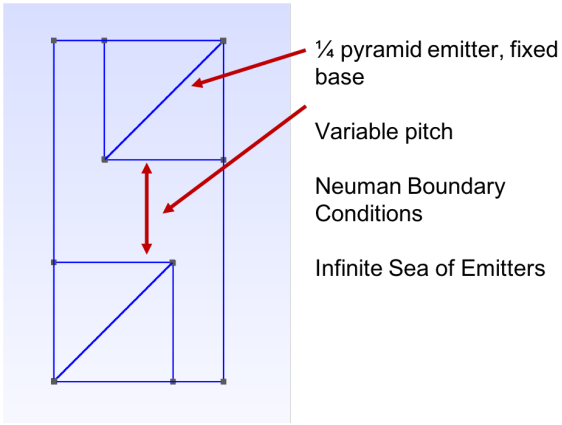

Fig. 9. To conduct initial models of tip shielding, we construct a unit array containing two quarter-pyramid emitters with fixed base size and variable pitch, matched with Neuman boundary conditions to form in infinite sea of emitters. Pitch is then varied while observing simulated per-tip emitted current.

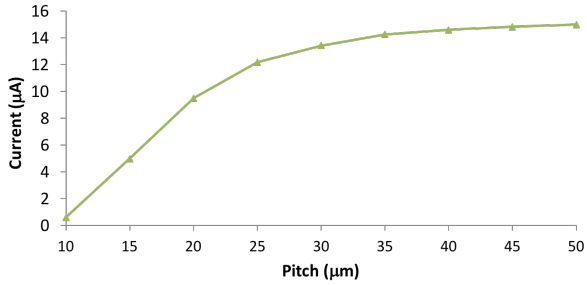

Fig. 10. Initial plot of per-tip emitted current as a function of tip spacing. Notice that current does not increase significantly for pitches larger than about 25 μm spacing for these 7 μm base pyramids.